

1

Bernard-Papineau_v10n6_Elements

2

Graphitic carbons and biosignatures

3

4

Sylvain Bernard¹ and Dominic Papineau²

5

Institut de Minéralogie, de Physique des Matériaux, et de Cosmochimie (IMPMC) - Sorbonne

6

Universités - MNHN, UPMC Univ Paris 06, CNRS UMR 7590, IRD UMR 206, 75005 Paris,

7

France, email: sbernard@mnhn.fr

8

²London Centre for Nanotechnology and Department of Earth Sciences, University College

9

London, 17-19 Gordon Street, London, WC1H 0AH, United Kingdom, email:

10

d.papineau@ucl.ac.uk

11

Box 1: Glossary of terms

12

Aliphaticity: Proportion of aliphatics in a molecule. Aliphatic groups are groups of carbon atoms joined together in straight chains, branched chains, or non-aromatic rings.

13

14

Archean: The Archean Eon is one of the five eons of Earth history. It starts after the Hadean eon (4 Ga) and ends with the beginning of the Proterozoic Eon (2.5 Ga). It is subdivided chronologically into four eras: the Eoarchean era, the Paleoarchean era, the Mesoarchean era and the Neoarchean era.

15

16

17

Aromaticity: Proportion of aromatics in a molecule. Aromatic groups are groups of carbon atoms arranged in rings with saturated and unsaturated bonds alternating in a particular way so that they follow Huckel's aromaticity law.

18

19

20

Biosignature: Morphological, elemental, molecular or isotopic feature inherited from life and preserved in rocks. Note that some biosignatures can potentially be mimicked by non-biological processes and should thus be considered less reliable and/or be supported by independent biosignatures.

21

22

23

Diagenesis: Collection of chemical, biological and physical post-depositional processes involved in the lithification of unconsolidated sediments into rocks at shallow depths and low temperatures (<200°C).

24

25

26

Fischer-Tropsch Type synthesis: Chemical reactions that convert a mixture of gaseous carbon oxides (e.g. CO, CO₂, HCO₃⁻, etc) and di-hydrogen into hydrocarbons through the catalytic effect of some transition metals (e.g. Ni, Cr, Fe, etc.).

27

28

29

Indigenicity/Syngenicity (or Indigeneity/Syngeneity): quality for graphitic carbons having been incorporated into sediments at the time these sediments were forming (syngenetic) and still present in the rock that has formed from these sediments (indigenous).

30

31

32

Kerogen: After having long been used to describe all organic molecules capable of oil generation, the term kerogen is now defined as the insoluble macromolecular organic matter that can be found in sedimentary rocks, regardless its biogenic or abiotic origin.

33

34

35

Organic biomarker: Class of biological organic molecules, typically from cellular membranes of living organisms, and their geological equivalents found in the rock record.

36 *Box 2: Glossary of techniques*

37 **CLSM:** Confocal Laser Scanning Microscopy is a non-destructive high spatial resolution optical
38 microscopy technique used on a selected depth in the specimen and which exploits the fluorescent response
39 of minerals and organic molecules to a given laser wavelength to provide imaging contrast.

40 **EA:** Elemental Analysis is a destructive analytical technique that allows the quantitative determination of
41 light element abundances (H, C, N, O, S) using the combustion or thermal conversion pyrolysis of a solid
42 (e.g. rock powder) into a gas. When coupled to IRMS, this technique also allows the determination of
43 isotope compositions.

44 **EDS:** Energy Dispersive Spectroscopy is a non-destructive high spatial resolution technique used to
45 determine chemical compositions using characteristic X-ray emitted from the impact of high-energy
46 electrons on a solid surface. Electron microscopes and microprobes are generally fitted with an EDS
47 detector.

48 **FIB-SEM:** Focused Ion Beam – Scanning Electron Microscopy is a minimally-destructive high spatial
49 resolution technique typically used to mill through a target for 3-D reconstructions or micro-fabrication of
50 ultrathin foils for TEM or STXM imaging.

51 **FTIR:** Fourier Transform InfraRed microscopy is a non-destructive high spatial resolution technique used
52 to spectroscopically map chemical bonds in minerals and organic molecules.

53 **GC-MS:** Gas chromatography – mass spectrometry is a destructive and highly sensitive technique that uses
54 a capillary column to separate gaseous molecules and then measures their molecular weight for
55 identification.

56 **IRMS:** Isotope Ratio Mass Spectrometry is a destructive technique that quantitatively measures the relative
57 abundance of stable and radiogenic isotopes to trace fractionation processes or dating.

58 **NanoSIMS:** Nanoscale Secondary Ion Mass Spectrometry is a minimally-destructive high spatial
59 resolution technique that quantitatively measures the abundance of isotopes.

60 **NMR:** Nuclear Magnetic Resonance is a non-destructive radio frequency spectroscopy technique that
61 quantitatively measures the chemical shift of isotopes with an odd number of protons or neutrons which
62 depends on its chemical bonding environment.

63 **Raman:** Laser Raman microspectroscopy is a non-destructive high spatial resolution technique used to
64 acquire diagnostic spectra from minerals and organic compounds that have a Raman response to an incident
65 beam of monochromatic photons.

66 **SEM:** Scanning Electron Microscopy is a non-destructive high spatial resolution technique that allows
67 imaging of solids using a range of quantum effects under high-energy electron bombardment. SEM
68 imaging is generally performed using secondary electrons, which give a depth of field created by the
69 relative number of secondary electrons detected as a function of the angle between the surface and the
70 electron beam, or using back-scattered electrons, where increased contrast is given by increasing atomic
71 numbers of the atoms composing the target.

72 **SIMS:** Secondary Ion Mass Spectrometry is a minimally-destructive high spatial resolution technique that
73 quantitatively measures the abundance of isotopes.

74 **STXM:** Scanning Transmission X-ray Microscopy is a non-destructive, high spatial resolution, and
75 synchrotron-based microscopy technique that allows collecting images with a contrast based on atomic
76 speciation and spectroscopy. Imaging is performed using the X-ray absorption near edge structure
77 (XANES) spectra of an element of interest, which offer insights into the local electronic structure of atoms
78 and allows the identification of chemical bonds.

79 **TEM:** Transmission Electron Microscopy is a non-destructive high spatial resolution technique that allows
80 imaging of ultrathin electron-transparent specimens. Contrast is given by the variable absorption of
81 electrons transmitted through the specimen caused by its chemical composition or thickness. TEM allows
82 bright-field imaging, High-Angle Annular Dark Field (HAADF) imaging, selected area electron diffraction
83 and EDS analyses.

84 **ToF-SIMS:** Time-of-Flight Secondary Ion Mass Spectrometry is a minimally-destructive high spatial
85 resolution technique that quantitatively measures the abundance of isotopes and molecule (with up to
86 10,000 amu).

87 **Abstract (<100 words)**

88 **Unambiguous identification of graphitic carbons as remains of life in ancient rocks**
89 **is challenging because fossilized biogenic molecules are inevitably altered and**
90 **degraded during diagenesis and metamorphism of the host rocks. Yet, recent studies**
91 **have highlighted the possible preservation of biosignatures carried by some of the**
92 **oldest graphitic carbons. Laboratory simulations are also increasingly used to better**
93 **constrain the transformations of organic molecules into graphitic carbons induced**
94 **by sedimentation and burial processes. These recent research advances collectively**
95 **justify a reevaluation of the putative biogenicity of numerous ancient graphitic**
96 **carbons, including the presumed oldest traces of life on Earth.**

97

98

99 **Keywords:**

- 100 - Microfossils
- 101 - Degradation/Preservation
- 102 - Diagenesis/Metamorphism
- 103 - Experimental Fossilization
- 104 - Abiotic Processes
- 105 - Archean/Early Life
- 106

107 **Introduction**

108

109 The search for evidence of early life in the geological record has often involved graphitic
110 carbons and has been a subject of intense debates and dividing controversies (e.g.,
111 Mojzsis et al. 1996; Rosing 1999; Schopf et al. 2002; Brasier et al. 2002; van Zuilen et al.
112 2003). Numerous challenges exist such as contamination and consideration of abiotic
113 pathways that may lead to the formation of graphitic carbons, which can be difficult to
114 distinguish from fossilized biological remains (Pasteris and Wopenka 2003; McCollom
115 and Seewald 2006). The main complication resides in the generally poor preservation of
116 biosignatures in the oldest metasedimentary rocks. Bio-alteration processes, as well as the
117 increase of temperature and pressure conditions during burial inevitably alter the original
118 biochemical signatures of organic molecules. As a result, the general paleobiological
119 perception has long been that burial processes are detrimental to the preservation of
120 signatures of life by graphitic carbons (see also Schiffbauer et al. 2007). However,
121 although numerous challenges still remain, newly available micro-analytical techniques
122 create innovative opportunities for the assessment of the biogenicity of graphitic carbons.

123

124 This contribution begins with an overview of the processes involved in the conversion of
125 biogenic organic molecules into graphitic carbons. Remarkable examples of exceptional
126 preservation of biosignatures by graphitic carbons in metasedimentary rocks are then
127 described. Possible solutions and new approaches to evaluate the biogenicity of graphitic
128 carbons are then explored. Finally, the question of the putative biogenicity of some Eo-
129 and Paleoarchean graphitic carbons is discussed in light of a selection of emblematic
130 examples from the recent literature.

131

132 **1. Conversion of organic biological remains into graphitic carbons**

133

134 When living organisms die, their organic molecules are usually rapidly biodegraded.
135 Most biomolecules released to the ambient environment are either oxidized or assimilated

136 by living microbes. Yet, some organic macromolecules resistant to biodegradation may
137 escape the biological cycle and get incorporated in sediments by selective preservation.
138 For instance, some labile organic molecules may bypass biodegradation through
139 degradation/recondensation reactions (e.g., Vandenbroucke and Largeau 2007).
140 Adsorption on inorganic surfaces as well as encapsulation within mineral microcavities
141 or larger molecules have also been reported as processes permitting the incorporation of
142 organic molecules into sediments (e.g., Vandenbroucke and Largeau 2007). The
143 respective contribution of each of these processes remains debated. Of note, organic
144 molecules incorporated into sediments through selective preservation, adsorption, or
145 encapsulation have likely only been slightly degraded and may still thus be identified. In
146 contrast, labile molecules incorporated into the sediments through
147 degradation/recondensation reactions have become geopolymers that may exhibit
148 chemical signatures distinct from those of the initial biomolecules. All these processes
149 lead to the formation of insoluble polymeric sedimentary organic macromolecules,
150 collectively called kerogen (Vandenbroucke and Largeau 2007).

151

152 Subsequent diagenetic processes may further complicate the recognition of biosignatures
153 (Figure 1). Partially preserved biosignatures carried by kerogen may suffer from
154 compaction and fluid migration. As fluid migration is limited within low permeability
155 sediments, they tend to favor the preservation of isotopic, elemental and molecular
156 biosignatures, whereas with high permeability sediments are unlikely to preserve
157 indigenous biosignatures (e.g., Vandenbroucke and Largeau 2007). During burial,
158 reducing sediment may minimize redox reactions with biogenic organic matter and
159 improve its preservation potential, through kerogen sulfurization for example (e.g.,
160 Vandenbroucke and Largeau 2007).

161

162 When burial increases, sedimentary rocks experience metamorphism at increasing
163 temperature and pressure conditions. The general paleobiological perception has long
164 been that burial-induced biomolecule degradation processes (carbonization/graphitization
165 processes) are detrimental to the morphological and chemical preservation of life remains
166 in rocks (Figure 1).

167

168 With increasing temperature conditions, the weaker bonds in kerogen molecules are
169 thermally broken and dehydrogenation reactions become predominant, leading to the
170 formation of graphitic carbons. Metamorphic degradation of kerogen is associated with
171 an increase in aromaticity and the release of heteroatoms such as O, N or S. By
172 promoting structural reorganization, thermal metamorphism may ultimately lead to pure
173 graphite that may have completely lost its original biosignatures. Finally, graphitic
174 carbons remain susceptible to late oxidation and hydrogenation, as well as to alteration or
175 contamination by younger biological carbon from the subsurface (particularly if carried
176 by groundwater) during exhumation processes.

177

178 Biogenic organic molecules may thus experience multiple stages of degradation induced
179 by a combination of biological, chemical, and physical factors during the geological
180 history of their host rocks. Yet, it has been demonstrated that products released by
181 kerogen degradation (i.e., thermally matured bitumen, molecular fossils and organic
182 biomarkers) may sometimes preserve structural information diagnostic of biological and
183 environmental provenance (e.g., Vandembroucke and Largeau 2007). This can also be the
184 case for graphitic carbons, as detailed in the following section.

185 **2. Preservation of biosignatures by natural graphitic carbons**

186

187 In contrast to the general belief, graphitic fossil occurrences in metamorphic rocks are
188 relatively common. The literature conceals a number of examples of graphitic fossils that
189 can be found in rocks of various ages and metamorphic facies, including the greenschist
190 facies (e.g., Butterfield et al. 2007), the amphibolite facies (e.g., Schiffbauer et al. 2007)
191 and the blueschist facies (e.g., Galvez et al. 2012). Notably, most of the metamorphic
192 fossils reported in the literature are organic-walled microfossils such as spores, dyncysts
193 or ‘acritarchs’, the latter being an emblematic graphitic fossil from the Proterozoic.

194

195 Numerous 'soft-bodied' fossils made of graphitic carbons have been described. Some of
196 the most illustrative examples undoubtedly include the graphitic fossils found in the
197 Middle Cambrian Burgess Shale Formation in the Rocky Mountains of southern British
198 Columbia, Canada (Figure 2). This formation is composed of calcareous mudstones and
199 limestones, and has experienced greenschist facies metamorphism at burial depths around
200 10 kilometers (Powell 2003). Yet, the Burgess fossil assemblage constitutes one of the
201 most diverse records of Cambrian animal life. Soft-bodied fossils from the Burgess Shale
202 that are preserved as graphitic films or graphitic carbonaceous compressions are reliably
203 interpreted as the remains of relatively recalcitrant organic exoskeletons, whereas those
204 preserved in three dimensions, via early diagenetic mineralization, typically represent
205 more labile cellular tissues (Butterfield et al. 2007). Although the mechanisms that
206 allowed their exceptional preservation remain debated, recent investigations have
207 evidenced the preservation of chitin molecular signatures in some of these fossils (Ehrlich
208 et al. 2013).

209

210 Also remarkable is the reported morphological preservation of graphitic plant
211 macrofossils in Mesozoic blueschist metamorphic rocks from the Marybank formation in
212 New Zealand (Galvez et al. 2012). Although these rocks have experienced burial to a
213 minimum depth of 15 km, fossil leaves and stems can be unambiguously identified.
214 Graphitic polygonal structures coated with micas may represent original cellular
215 ultrastructure. Yet, despite the excellent morphological preservation, organic biomarkers
216 and molecular functional groups of these graphitic carbons have been completely lost
217 during metamorphism.

218

219 Other spectacular, morphologically preserved graphitic fossils are lycophyte megaspores
220 from Triassic metasedimentary carbonate concretions from Vanoise in the western Alps,
221 France (Figure 3 - Bernard et al. 2007). These partially mineralized microfossils
222 experienced blueschist facies metamorphism ($\sim 360^{\circ}\text{C}$, $\sim 14\text{kbars}$, i.e. a burial depth of
223 about 40 km) during the late Mesozoic and Cenozoic Alpine Orogeny. While mainly
224 composed of graphitic carbons, these microfossils exhibit chemical and structural
225 heterogeneities, which have been interpreted as remnants of original biochemical signals.

226 In particular, the chemical signature of degraded sporopollenin, the resistant biopolymer
227 composing modern spore and pollen grain walls, has been identified within the fossilized
228 megaspore walls using synchrotron-based STXM and XANES spectroscopy (Bernard et
229 al. 2007).

230

231 Thus, the preservation of micro- to macroscale morphologies and of some molecular
232 information in graphitic microfossils may not be as extraordinary as generally believed.
233 Still, original biosignatures carried by organic molecules are degraded at least partially, if
234 not completely, during bio-alteration and burial processes. Therefore, unambiguously
235 identifying fossils of microorganisms in ancient rocks remains a challenging goal. As
236 detailed in the following section, the next step to adequately interpret the ancient organic
237 fossil record lies in quantitatively constraining the impact of bio-alteration and burial
238 processes on organic molecule degradation.

239

240 **3. Experimental fossilization**

241

242 Although laboratory simulations do not perfectly simulate natural diagenesis,
243 experimental investigations are increasingly seen as a promising route towards
244 quantitative analyses of the transformations of organic molecules induced by burial
245 processes. Most of the recent attempts of experimental fossilization have aimed at
246 reproducing and better constraining early diagenetic processes that contribute to the
247 morphological preservation of organic structures (e.g., Li et al. 2013). Yet, numerous
248 studies are now also aimed at exploring the molecular evolution of organic molecules
249 during artificial maturation (e.g., Li et al. 2013; Figure 4).

250

251 The use of isotope compositions to evaluate the biogenicity of graphitic carbons appears
252 necessary but insufficient. Abiotic pathways such as the decarbonation of siderite and
253 Fischer-Tropsch Type synthesis (FTT) are known to produce organic molecules with
254 isotopic signatures similar to those of biological carbons, *i.e.* depleted in ^{13}C (McCullom
255 and Seewald 2006). Recent hydrous pyrolysis experiments on kerogen in isotopically-

256 labeled aqueous solutions have shown that temperature increase promotes isotopic
257 exchange between macromolecular organic matter and reactive inorganic compounds
258 (Schimmelman and Lis 2010). Kinetic extrapolation from long experiments performed at
259 100°C suggests that isotopic exchange may even be significant in natural settings at
260 temperatures as low as 40-50°C. Although, isotopic re-equilibration is not ineluctable,
261 such modifications of isotopic signatures may lead to erroneous interpretations that
262 would jeopardize the search for early life in the geological record.

263

264 Structural and molecular biosignatures appear a bit more robust. For instance, using
265 heating experiments to simulate organic matter thermal alteration, Schopf et al. (2005)
266 showed that Raman spectroscopy may provide sensitive indicators of the low-temperature
267 alteration of graphitic carbons. More, recently, Schiffbauer et al. (2012) exposed natural
268 fossilized acritarchs from the Mesoproterozoic Ruyang Group to experimental heating at
269 approximately 500°C for up to 250 days, in both oxic and anoxic conditions. Notably,
270 anoxic replicates retain biological morphologies despite an increasing degree of
271 carbonization with continuous heating. In contrast, oxic replicates experienced more
272 aggressive degradation when submitted to the same time/temperature conditions.
273 Following a similar approach, Li et al. (2013) have investigated the structural and
274 chemical transformations of bacterial cells during thermal aging experiments performed
275 under anoxic conditions. Combined microscopy and spectroscopy data demonstrate
276 partial morphological and chemical preservation of bacterial cells completely encrusted
277 by iron phosphates despite heating treatments at hundreds of degrees for several hours
278 under argon atmosphere. This study illustrates that inorganic phases may favor
279 morphological and chemical preservation during carbonization processes.

280

281 Altogether, the trends in chemical, structural and isotopic changes reported in
282 experimental fossilization studies provide new milestones towards a generalized
283 mechanistic model of organic molecule degradation processes occurring during
284 diagenesis and metamorphism. In addition to simulating biodegradation and taphonomic
285 processes in the laboratory, future studies should investigate the impact of key parameters
286 such as the geochemical nature of the fluid and the mineral matrix on the extent of

287 biomolecule degradation occurring during burial in natural settings. Artificial maturation
288 experiments performed in open or closed systems under well-constrained physical and
289 chemical conditions have been extensively used for decades to better constrain kerogen
290 degradation processes (e.g., Vandenbroucke and Largeau 2007). In addition, the recent
291 development of advanced characterization techniques allow the evolution of chemical,
292 structural and isotopic signatures of graphitic carbons within natural maturation series to
293 be precisely documented (Bernard et al. 2014).

294 **4. Controversies over the earliest traces of life**

295

296 Although many claims for Eoarchean and Paleoarchean life have been made on the basis
297 of graphitic carbons, many controversies have arisen regarding their origin (e.g., Mojzsis
298 et al. 1996; Rosing 1999; Schopf et al. 2002; Brasier et al. 2002; van Zuilen et al. 2003).
299 Because of the inevitable alteration of organic molecules that occurs during burial,
300 biogenic graphitic carbons can be difficult to differentiate from carbons coming from
301 contamination. Contamination in geological specimens may have several origins: (1) an
302 experimental origin where samples are contaminated during sampling, handling, and/or
303 preparation; and (2) a natural origin where samples may be contaminated by natural
304 abiotic carbons or younger biogenic carbons during fluid migration or biodegradation.
305 Because of these difficulties, the distinction of biogenic from non-biogenic graphitic
306 carbons in Archean rocks remains an open issue.

307

308 Here we propose a series of criteria, listed in Table 1, to be considered when
309 investigating the possible biological origin of Eo- and Paleoarchean graphitic carbons in
310 order to prevent misinterpretations. For instance, the occurrence of ^{13}C -depleted
311 diamonds and graphitic carbons included in Hadean zircons from the Jack Hills in
312 Western Australia has been interpreted as possible evidence of the earliest carbon cycle
313 and/or early life (Menneken et al. 2007). Yet, nanoscale TEM observations performed on
314 foils micro-fabricated by focused ion beam (FIB) have recently revealed that the
315 observed graphite-diamond mixtures included in the Hadean zircons are embedded in

316 epoxy, leading to the conclusion that they are contaminants from polishing compounds
317 during sample preparation (Dobrzhinetskaya et al. 2014).

318

319 Among other controversial findings is the isotopically light graphite (with $\delta^{13}\text{C}$ values
320 between -21 and -49‰) reported as inclusions within apatite crystals and interpreted to
321 be the oldest signs of life from ca. 3.83 Ga granulite facies quartz-pyroxene (Qp) rock on
322 the Island of Akilia, Southwest Greenland (Mojzsis et al. 1996). It has been argued that
323 because these graphitic particles are completely included within apatite crystals, their
324 isotopic signatures could not have resulted from isotope exchanges with fluids during
325 long crustal residence times (Mojzsis et al. 1996). Yet, laboratory demonstration that
326 abiotic hydrothermal pathways, such as siderite decarbonation and Fischer-Tropsch–Type
327 (FTT) synthesis, may lead to the formation of carbonaceous compounds depleted in ^{13}C
328 (McCollom and Seewald 2006) have led to question the biogenic origin of these graphite
329 particles. In addition, recent nanoscale investigations performed on FIB foils have
330 revealed clear evidence for fluid-deposited graphite particles in the Akilia Qp rocks
331 (Figure 5a), rather present as coatings on apatite grains and not demonstrably as
332 inclusions (Figure 5b - Papineau et al. 2010a). The graphite from this rock has been
333 further shown by two other independent analytical methods to have $\delta^{13}\text{C}$ values between -
334 4.1 and -23.6‰ and thus are not as fractionated as previously reported (Papineau et al.
335 2010b). Although H, O, N, S and P have all been detected in this graphite, recent
336 nanoscale observations by FIB of graphite coatings on apatite grains within the banded
337 iron formations from the ca. 3.75 Ga old Nuvvuagittuq Supracrustal Belt have shown that
338 such mineral association can be fluid-deposited during the late history of the rock
339 (Papineau et al. 2011). This example illustrates the importance of unambiguously
340 demonstrating indigenicity before discussing the age and biogenicity of graphitic
341 carbons.

342

343 Graphite particles from the ca. 3.77 Ga turbiditic schists from the Isua Supracrustal Belt
344 have also been interpreted as biogenic remains based on their abundance and isotopic
345 signatures (Rosing 1999). Yet, additional measurements showing less ^{13}C -depleted
346 graphite particles in Isua metacarbonate rocks have led to an interpretation of these

347 particles as resulting from the abiotic thermal decarbonation of siderite (van Zuilen et al.
348 2003). Since then, turbiditic schists from Isua have been reported to contain graphitic
349 layers with highly variable graphite content (from 5 up to 10 wt %) and $\delta^{13}\text{C}$ values (from
350 -15‰ down to -24‰). Such values have been interpreted as consistent with a biogenic
351 origin (Ohtomo et al. 2014). However, these recent interpretations remain debated,
352 notably because they rely on samples from a unique formation.

353

354 Perhaps the most famous report of graphitic microfossil evidence for earliest life is the
355 discovery of microbial-like structures composed of graphitic carbon from the ca. 3.46 Ga
356 Apex chert in the Warrawoona Group (Schopf et al. 2002). While these microscopic
357 objects were originally interpreted as cyanobacterial microfossils and subsequently
358 became the benchmark for *bona fide* Paleoproterozoic microfossils, their biogenic origin has
359 come into question after re-examination of their morphology and their geological and
360 geochemical context (Brasier et al. 2002). Recent investigations have demonstrated that
361 these objects are composed of variably graphitized carbons that contain molecular
362 functional groups and heteroatoms of N, S, and P that would suggest a biological origin
363 (De Gregorio et al. 2009). Yet, the origin of this graphitic carbon is still debated, with
364 interpretations for their origin varying from Fischer-Tropsch Type (FTT) synthesis
365 (Brasier et al. 2011) to contamination by younger organic matter (Olcott Marshall et al.
366 2012). Additional support to better assess the origin of these microscopic objects may
367 come from similar analyses on graphitic carbons from other rocks of similar age (e.g.
368 Table 1). For instance, Wacey et al. (2012) have recently concluded on the biogenicity of
369 microfossil-like structures containing spheroidal nano-grains of silica embedded in
370 graphitic carbon from the 3.35 Ga Strelley Pool formation. Yet, their conclusions mostly
371 rely on the morphological similarities that these objects share with Gunflint microfossils
372 as observed using FIB-SEM and TEM. The Strelley Pool formation is the target of a
373 number of investigations as it hosts different types of graphitic carbons (Figure 5c) as
374 well as stromatolites (Figure 5d).

375

376

4. Remaining questions and concluding remarks

377

378

379 The controversies detailed above highlight the need for a great deal of caution to be
380 implemented to gather the multiple lines of evidence that may allow the unambiguous
381 identification of ancient graphitic carbons as biological remains. Yet, a series of
382 fundamental questions still needs to be addressed.

383

384 For instance, almost nothing is known regarding the possibility that abiotic carbons
385 accumulate as aromatic compounds and polymerize within sediments or sedimentary
386 rocks. FTT synthesis generally proposed as the source of controversial graphitic carbons
387 dominantly produces short aliphatic hydrocarbons (McCollom and Seewald 2006). The
388 fate of such abiotic organic molecules in sedimentary rocks over geological time-scales
389 indeed remains totally unknown. Under what conditions can these hydrocarbon chains
390 become aromatic macromolecules, difficult to distinguish from graphitic carbons
391 resulting from the degradation of organic molecules of biogenic origin? What geological
392 mechanisms and conditions would have to work in concert to yield accumulations of
393 abiotic poorly crystalline graphitized carbon from such aliphatic precursors? What type
394 of FTT synthesis or diagenetic pathways could produce poorly graphitic microbial-like
395 features?

396

397 Galvez et al. (2013) reported graphite formation from abiotic calcite reduction at low
398 temperature in an exhumed serpentinite-sediment contact in Alpine Corsica (France).
399 Based on isotopic and spectroscopic measurements, these authors argued that this
400 graphite has formed from an abiotic source of carbon and could be distinguished from the
401 biogenic graphitic carbons observed in the same rocks. Yet, such reports of robust
402 geochemical evidence for geological deposits of abiotic graphitic carbons remain quite
403 scarce, in contrast to what should be expected based on the null hypothesis. In the present
404 context, the null hypothesis stipulates that all possible abiotic pathways need to be
405 disproven before a biogenic origin can be accepted. This cautionary approach certainly
406 deserves merits for the oldest sedimentary rocks and in an exobiological context.
407 However the null hypothesis could likewise be used in the opposite way as far as

408 terrestrial organic matter is concerned, from a uniformitarian perspective. Ultimately,
409 such debates are healthy for this field of science as they stimulate additional research and
410 can only be solved by using new analytical approaches and sample suites.

411

412 Altogether, all these questions can be summarized in a single question: “*How can ancient*
413 *graphitic carbon be unambiguously assigned an origin?*”. This apparently trivial question
414 is full of hidden fundamental and methodological issues. Table 1 is an attempt at listing
415 criteria that should be fulfilled in order to unambiguously assign a biogenic origin to
416 graphitic carbons of Eoarchean or Paleoarchean age. Undoubtedly, a great deal of caution
417 is required to prepare samples for micro-analyses and to gather the multiple lines of
418 evidence that may eventually lead to the identification of ancient graphitic carbons as
419 biological remains. In addition, we suggest here that identification of biogenic graphitic
420 carbons in ancient rocks should not be based on results obtained from a single locality.
421 Most importantly, the determination of syngenicity and indigenicity of putative
422 microfossils and/or graphitic carbons within metasedimentary rocks requires a precise
423 assessment of the thermal history that they have experienced, as well as quantitative
424 constraints on the biosignatures that may be preserved by these graphitic carbons in light
425 of their thermal history. Development of experimental fossilization shall allow substantial
426 progress in that regard in the future.

427

428 As described here, the assessment of the origin of graphitic carbons in ancient rocks
429 remains challenging and debatable since the behaviors of biogenic and abiotic carbons
430 during diagenesis and metamorphism have not yet been precisely constrained. Likewise,
431 while there remain uncertainties about the possible biogenic origin of graphitic carbons in
432 Eo- and Paleoarchean metasedimentary rocks, significant advances have recently been
433 made with the introduction of new micro-analytical techniques. Such tools have helped to
434 expand databases and generate reproducible observations of samples from ancient
435 sedimentary rocks. Such progress opens up new sub-fields in Precambrian micro-
436 paleontology and nanobiogeochemistry and holds great promise to contribute to the
437 current challenges of addressing the origin of graphitic carbons.

438

439 Table 1: list of suggested criteria for graphitic carbons that need to be satisfied in order to
 440 assign a biogenic origin to graphitic carbons.

	Required criteria	Cautionary notes	Techniques useful for assessment*
Geological context	Sedimentary nature of the protolith	Chemical sediments might have formed in multiple generations and under the seafloor or in the crust.	Field studies, geological, petrological and/or geochemical studies.
Petrographic context	Occurrences of graphitic carbons should be numerous within a single thin section and demonstrably indigenous. Morphological and textural structures may be important clues but may not be unambiguous.	Possible artefacts resulting from sample preparation and other sources of contamination should be identified and avoided.	Macroscopic observations, Optical microscopy, CLSM, Raman, SEM, EA.
Mineralogical context	Graphitic carbon occurrences should be included within the crystalline mineral matrix and not in pore spaces.	Occurrences associated with neoformed minerals, alteration and skarn phases should be investigated with special care.	Optical microscopy, Raman, FTIR, FIB-SEM, TEM-EDS.
Structural and microstructural characteristics	Proofs of syngeneity: the crystalline structure of the graphitic carbon is consistent with the peak metamorphic conditions experienced by the host rock.	Care is need for host rocks that have experienced a multi-phase geological history.	Raman, FTIR, STXM, TEM-based electron diffraction.
Isotopic composition	¹³ C-depleted carbon isotopic compositions consistent with biological origin, taking into account the possible metamorphic fractionation and re-equilibration of	Adequate standards should be used, and artefacts should be identified and avoided. Care is also needed as non-biogenic carbons	IRMS, SIMS, NanoSIMS.

	inorganic carbon phases.	may exhibit similar values.
Elementary composition	Graphitic carbons of biogenic origin might still contain heteroatoms (O, N, P, S) as traces.	Contamination by recent carbon, if any, should be identified.
Molecular Structure	Trace levels of molecular functional groups might remain present and be consistent with heteroatom content.	Their amount should be consistent with the thermal history of the host rock
Reproducible Observations	Reproducible observations in other samples from other localities appear necessary.	Absence of evidence is not evidence of absence

441 *List of abbreviations: IRMS is Isotope Ratio Mass Spectrometry, EA is Elemental Analysis, CLSM is
442 Confocal Laser Scanning Microscopy, FIB is Focused Ion Beam, TEM is Transmission Electron
443 Microscopy, EDS is Energy Dispersive Spectroscopy, SIMS is Secondary Ion Mass Spectrometry, ToF-
444 SIMS is Time-of-Flight Secondary Ion Mass Spectrometry, NanoSIMS is Nanoscale Secondary Ion Mass
445 Spectrometry, STXM is Scanning Transmission X-ray Microspectroscopy, GC-MS is Gas Chromatography
446 – Mass Spectrometry, NMR is Nuclear Magnetic Resonance.

447

448

449

450 **Acknowledgements**

451 SB acknowledges support from the ERC (project PaleoNanoLife - PI: F. Robert) and DP
452 acknowledges support from the University College London and the NASA Astrobiology Institute
453 (grant numbers NNA04CC09A, NNA09DA81A, and NNX12AG14G). STXM-based XANES
454 data shown on Figure 4 were acquired at beamlines 5.3.2.2 and 11.0.2 at the ALS, which is
455 supported by the Director of the Office of Science, Department of Energy, under Contract No.
456 DE-AC02-05CH11231. Special thanks go to David Kilcoyne and Tolek Tyliczszak for their
457 expert support on STXM at the ALS.

458

459

461 REFERENCES

- 462 Bernard S, Benzerara K, Beyssac O, Menguy N, Guyot F, Brown Jr GE, Goffe B (2007) Exceptional
463 preservation of plant fossils in high-pressure metamorphic rocks. *Earth and Planetary Science Letters*
464 262/1-2: 257-272
- 465 Bernard S, Horsfield B (2014) Thermal Maturation of Gas Shale Systems. *Annual Review of Earth and*
466 *Planetary Science* 42: 635-641.
- 467 Brasier MD, Green OR, Jephcoat AP, Kleppe AK, Van Kranendonk MJ, Lindsay JF, Steele A, Grassineau
468 NV (2002) Questioning the evidence for earth's oldest fossils. *Nature* 416(6876): 76-81
- 469 Brasier MD, Green OR, Lindsay JF, Mcloughlin N, Stoakes CA, Brasier AT, Wacey D (2011) Geology and
470 putative microfossil assemblage of the c. 3460 Ma 'Apex chert', Chinaman Creek, Western Australia -
471 A field and petrographic guide. Government of Western Australia, Department of Mines and
472 Petroleum, 65 pp. (V)
- 473 Butterfield NJ, Balthasar U, Wilson LA (2007) Fossil diagenesis in the Burgess Shale, *Palaeontology* 50:
474 537-543
- 475 De Gregorio BT, Sharp TG, Flynn GJ, Wirick S, Hervig RL (2009) Biogenic origin for Earth's oldest
476 putative microfossils. *Geology* 37: 631-634
- 477 Dobrzhinetskaya L, Wirth R, Green H (2014) Diamonds in Earth's oldest zircons from Jack Hills
478 conglomerate, Australia, are contamination. *Earth and Planetary Science Letters* 387: 212-218
- 479 Ehrlich H, Rigby JK, Botting JP, Tsurkan MV, Werner C, Schwille P, Petrask Z, Pisera A, Simon P,
480 Sivkov VN, Vyalikh DV, Molodtsov SL, Kurek D, Kammer M, Hunoldt S, Born R, Stawski D,
481 Steinhof A, Bazhenov VV, Geisler T (2013) Discovery of 505-million-year old chitin in the basal
482 demosponge *Vauxia gracilentia*. *Nature, Scientific Report* 3: 1-6
- 483 Galvez ME, Beyssac O, Benzerara K, Bernard S, Menguy N, Cox SC, Martinez I, Johnston MR, Brown Jr
484 GE (2012) Morphological preservation of carbonaceous plant fossils in high grade metamorphic rocks
485 from New Zealand. *Geobiology* 10(2): 118-129.
- 486 Galvez ME, Beyssa O, Martinez I, Benzerara K, Chaduteau C, Malvoisin B, Malavieille J (2013) Graphite
487 formation by carbonate reduction during subduction. *Nature Geoscience* 6: 473-477.
- 488 Li J, Benzerara K, Bernard S, Beyssac O (2013) The link between biomineralization and fossilization of
489 bacteria: Insights from field and experimental studies. *Chemical Geology* 359: 49-69
- 490 McCollom TM, Seewald JS, (2006) Carbon isotope composition of organic compounds produced by
491 abiotic synthesis under hydrothermal conditions. *Earth and Planetary Science Letters* 243(1-2): 74-84
- 492 Menneken M, Nemchin AA, Geisler T, Pidgeon RT, Wilde SA (2007) Hadean diamonds in zircon from
493 Jack Hills, Western Australia. *Nature* 448(7156): 917-20
- 494 Mojzsis SJ, Arrhenius G, McKeegan KD, Harrison TM, Nutman AP, Friend CRL (1996) Evidence for life
495 on Earth before 3,800 million years ago. *Nature* 384(6604): 55-59
- 496 Olcott Marshall A, Emry JR, Marshall CP (2012) Multiple Generations of Carbon in the Apex Chert and
497 Implications for Preservation of Microfossils. *Astrobiology* 12(2): 160-166
- 498 Ohtomo Y, Kakegawa T, Ishida A, Nagase T, Rosing MT (2014) Evidence for biogenic graphite in early
499 Archaean Isua metasedimentary rocks. *Nature Geoscience* 7: 25-28
- 500 Papineau D, De Gregorio BT, Cody GD, Fries MD, Mojzsis SJ, Steele A, Stroud RM, Fogel ML (2010)
501 Ancient graphite in the Eoarchean quartz-pyroxene rocks from Akilia in southern West Greenland I:
502 Petrographic and spectroscopic characterization. *Geochimica et Cosmochimica Acta* 74(20): 5862-
503 5883
- 504 Papineau D, De Gregorio BT, Stroud RM, Steele A, Pecoits E, Konhauser K, Wang J, Fogel ML (2010)
505 Ancient graphite in the Eoarchean quartz-pyroxene rocks from Akilia in southern West Greenland II:
506 Isotopic and chemical compositions and comparison with Paleoproterozoic banded iron formations.
507 *Geochimica et Cosmochimica Acta* 74(20): 5884-5905
- 508 Papineau D, De Gregorio BT, Cody GD, O'Neill J, Steele A, Stroud RM, Fogel ML (2011) Young poorly
509 crystalline graphite in the > 3.8-Gyr-old Nuvvuagittuq banded iron formation. *Nature Geoscience*
510 4(6) : 376-379
- 511 Pasteris JD, Wopenka B (2003) Necessary, but not sufficient: Raman identification of disordered carbon as
512 a signature of ancient life. *Astrobiology* 3(4): 727-738
- 513 Powell W (2003) Greenschist-facies metamorphism of the Burgess Shale and its implications for models of
514 fossil formation and preservation. *Canadian Journal of Earth Sciences* 40(1): 13-25

515 Rosing MT (1999) C-depleted carbon microparticles in >3700-Ma sea-floor sedimentary rocks from West
516 Greenland. *Science* 283 : 674-676

517 Schiffbauer JD, Yin LM, Bodnar RJ, Kaufman AJ, Meng FW, Hu J, Shen B, Yuan XL, Bao HM, Xiao SH
518 (2007) Ultrastructural and geochemical characterization of Archean-Paleoproterozoic graphite
519 particles: Implications for recognizing traces of life in highly metamorphosed rocks. *Astrobiology*
520 7(4): 684-704

521 Schiffbauer JD, Wallace AF, Hunter Jr JL, Kowalewski M, Bodnar RJ, Xiao SH (2012) Thermally-induced
522 structural and chemical alteration of organic-walled microfossils: An experimental approach to
523 understanding fossil preservation in metasediments. *Geobiology* 10(5): 402-423

524 Schimmelmann A, Lis GP (2010) Nitrogen isotopic exchange during maturation of organic matter. *Organic*
525 *Geochemistry* 41(1), 63-70

526 Schopf JW, Kudryavtsev AB, Agresti DG, Wdowiak TJ, Czaja AD (2002) Laser-Raman imagery of Earth's
527 earliest fossils. *Nature* 416(6876): 73-76

528 Schopf JW, Kudryavtsev AB, Agresti DG, Czaja AD, Wdowiak TJ (2005) Raman imagery: A new
529 approach to assess the geochemical maturity and biogenicity of permineralized Precambrian fossils.
530 *Astrobiology* 5(3): 333-371.

531 van Zuilen MA, Lepland A, Teranes J, Finarelli J, Wahlen M, Arrhenius G (2003) Graphite and carbonates
532 in the 3.8 Ga old Isua Supracrustal Belt, Southern West Greenland. *Precambrian Research* 126(3-4):
533 331-348

534 Vandenbroucke M, Largeau C (2007) Kerogen origin, evolution and structure. *Organic Geochemistry*
535 38(5): 719-833

536 Wacey D, Menon S, Green L, Gerstmann D, Kong C, McLoughlin N, Saunders M, Brasier M (2012)
537 Taphonomy of very ancient microfossils from the ~3400 Ma Strelley Pool Formation and ~1900 Ma
538 Gunflint Formation: New insights using a focused ion beam. *Precambrian Research* 220/221: 234-250
539
540
541

542 **FIGURE CAPTION**

543

544 **Figure 1:** *Illustration of the possible evolution of a living organism after its death during*
545 *diagenesis and metamorphism.*

546 **Figure 2:** *Photographs of Burgess shale graphitic soft-bodied fossils: a 5-centimeter*
547 *long Opabinia specimen (A) and a 2-centimeter long Hallucigenia specimen (B). Source:*
548 *Museum of Natural History, Smithsonian Institution (www.mnh.si.edu)*

549 **Figure 3:** *A: Reflected light photomicrograph of a fossilized megaspore found in Triassic*
550 *metamorphic rocks from the western French Alps (blueschist facies - 360°C - 14 kbars).*
551 *B: Corresponding Raman map showing the spatial distribution of graphitic carbon*
552 *(blue), calcite (red) and ankerite (yellow). C: XANES spectra of graphitic carbons*
553 *composing the wall of these objects and reference spectra of sporopollenin (the*
554 *biopolymer that constitutes modern spores and pollen grains walls), lignin and graphite.*
555 *The graphitic carbon composing the Vanoise megaspore wall is identified as degraded*
556 *sporopollenin (modified from Bernard et al. 2007).*

557 **Figure 4:** *Evolution of the XANES signal of lignin experimentally heat-treated under an*
558 *inert Argon atmosphere at different temperature up to 1000°C for 90 minutes (A) and for*
559 *different durations up to 900 minutes at 360°C (B). These data show a significant*
560 *increase of aromaticity and a net loss of heteroatom-containing functional groups with*
561 *increasing temperature and experimental duration.*

562 **Figure 5:** *A-B: Back-Scattered Electron images of graphite from the Eoarchean Akilia*
563 *Quartz-pyroxene rock showing fluid-deposited graphite (gra) indicated by mineral*
564 *associations with calcite (cal), magnetite (mag), chalcopyrite (ccp), pyrrhotite (po), and*
565 *enveloped in hornblende (A) and graphite coating on apatite (ap), also possibly fluid-*
566 *deposited (B). C: Crossed polar image of a globule of black graphitic carbon surrounded*
567 *by a halo of finely disseminated brown organic matter and euhedral dolomite (red arrow)*
568 *from a Paleoarchean chert in the Strelley Pool Formation. D: Small domal laminated*
569 *stromatolites from the Strelley Pool Formation (coin is 28.5 mm for scale).*

Living Organism

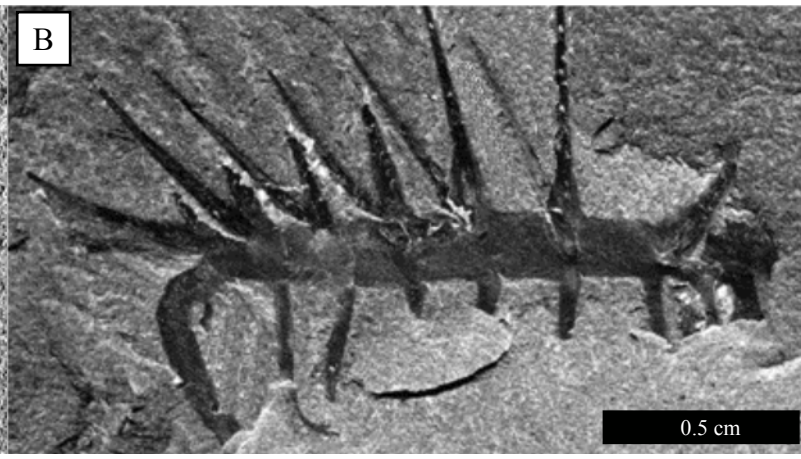
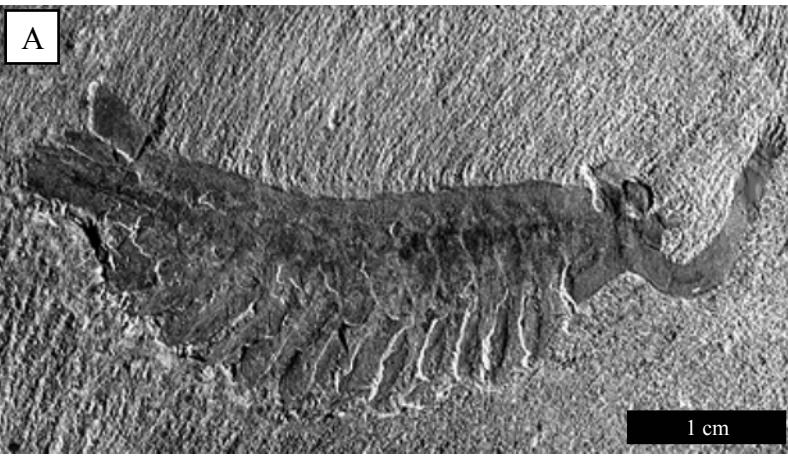


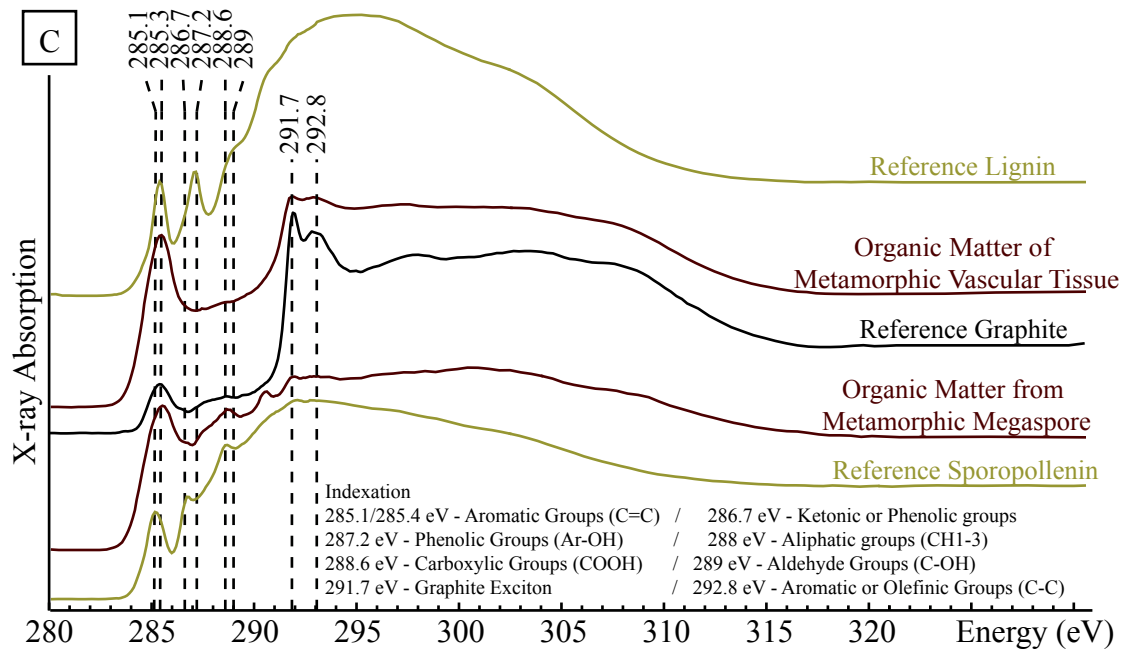
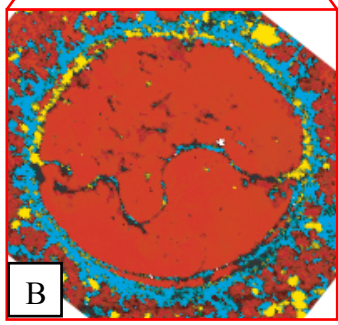
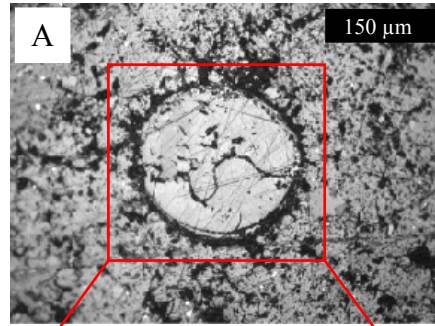
Sedimentary Rock

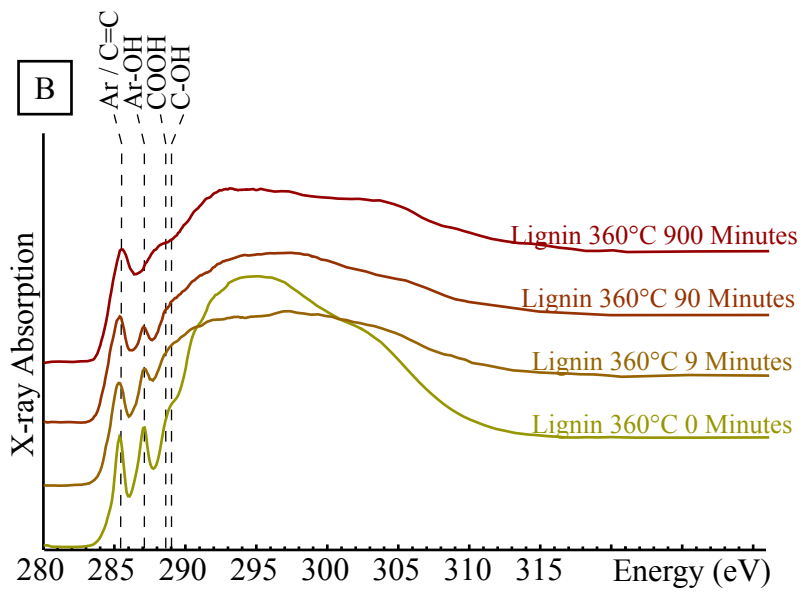
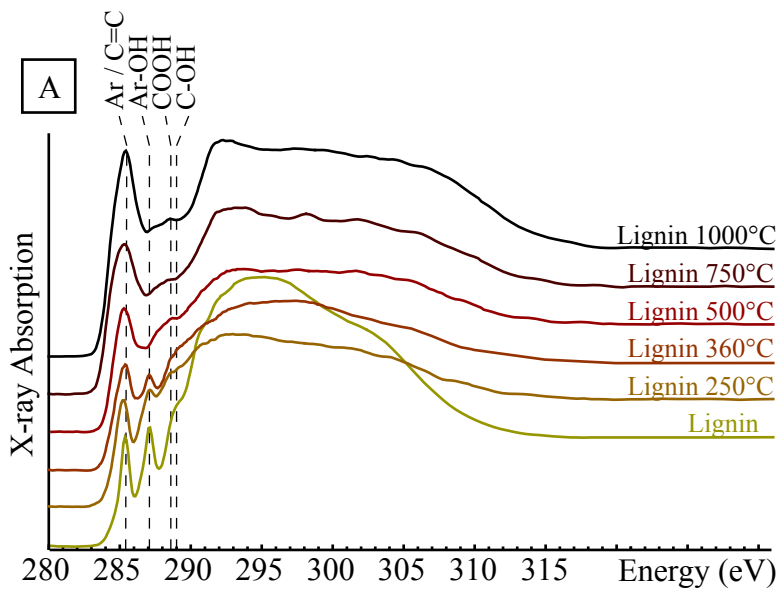


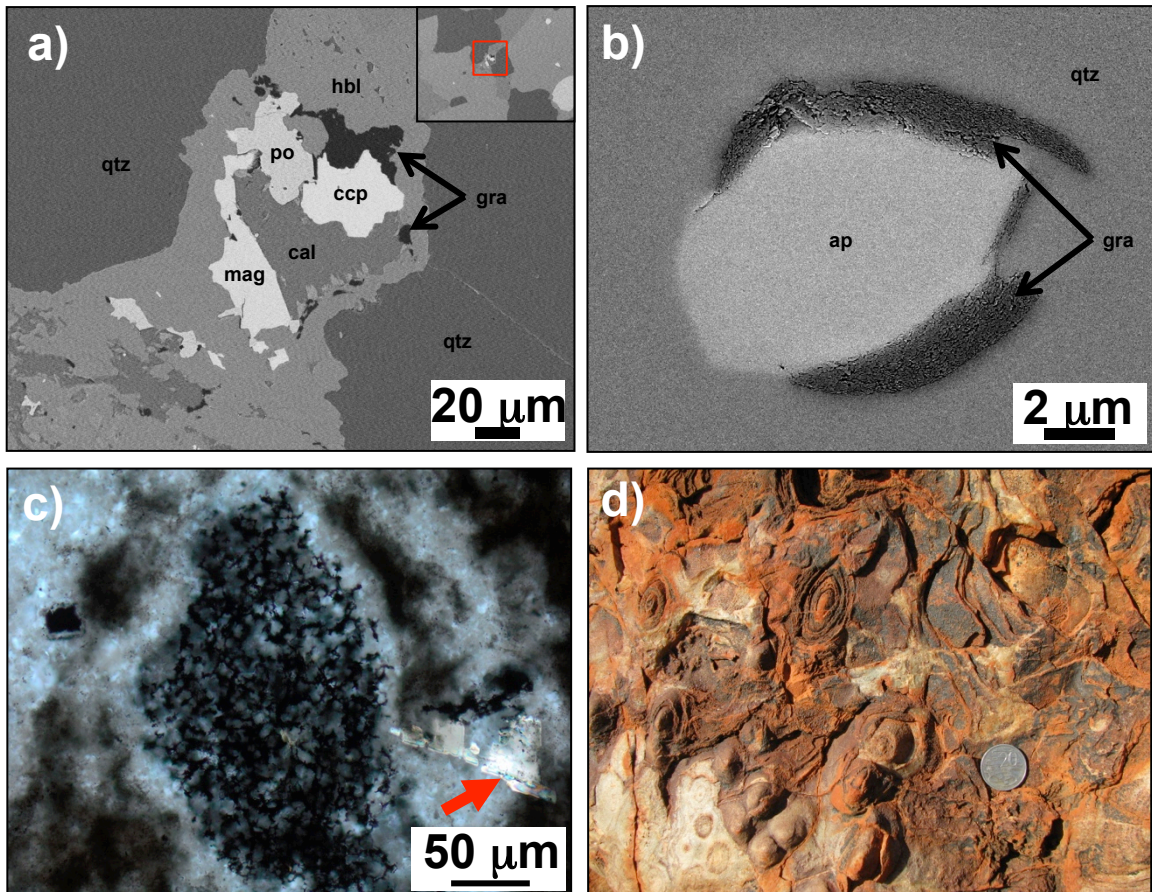
Metasedimentary Rock











Revised caption: a-b) Back-Scattered Electron images of graphite from the Eoarchean Akilia Quartz-pyroxene rock showing a) fluid-deposited graphite (gra) indicated by mineral associations with calcite (cal), magnetite (mag), chalcopyrite (ccp), pyrrhotite (po), and enveloped in hornblende and b) graphite coating on apatite (ap), also possibly fluid-deposited. c) Crossed polar image of a globule of black graphitic carbon surrounded by a halo of finely disseminated brown organic matter and euhedral dolomite (red arrow) from a Paleoarchean chert in the Strelley Pool Formation. d) Small domal laminated stromatolites from the Strelley Pool Formation (coin is 28.5 mm for scale).